Density Functional Calculations of Hyperfine Coupling Constants in Alanine-Derived Radicals

Philippe Lahorte,*,† Frank De Proft,‡,⊥ Gauthier Vanhaelewyn,§,∥ Bert Masschaele,† Peter Cauwels,† Freddy Callens,§,⊗ Paul Geerlings,‡ and Wim Mondelaers†

Department of Subatomic and Radiation Physics, Radiation Physics Group, Gent University, Proeftuinstraat 86, B-9000 Gent, Belgium, Member of IBITECH; Eenheid Algemene Chemie (ALGC), Free University of Brussels, Pleinlaan 2, B-1050 Brussels, Belgium, and Laboratory for Crystallography and Study of the Solid State, Gent University, Krijgslaan 281-S1, B-9000 Gent, Belgium

Received: March 17, 1999; In Final Form: June 18, 1999

We present the results of density functional calculations of ^{1}H, ^{13}C, and ^{14}N hyperfine coupling constants (hfcc's) in radicals derived from the simple amino acid L-alanine. The calculations are performed using the B3LYP functional in combination with Pople basis sets (6-31G(d) and 6-311G(d)) and the IGLO-III basis set. Both isotropic and anisotropic hfcc's show good agreement with available experimental data. Detailed study of the isotropic hfcc's allows for investigation of specific geometrical features of the various radical structures. The scope and limitations of this type of calculations both for elucidation of experimental electron paramagnetic resonance spectra and investigation of radical structure are briefly discussed.

1. Introduction

The amino acid L-α-alanine (see Figure 1) is one of the most intensively studied simple amino acids mainly because of the specific properties it displays in the solid state form. Especially its good dose yield factors, linear signal response over a wide dose range, excellent fading characteristics, and limited dependency on dose rate, radiation quality, and environmental factors, such as temperature and humidity, make it an ideal candidate for a wide range of applications in electron paramagnetic resonance (EPR) dosimetry.[1] As a result of extensive EPR and electron nuclear double resonance (ENDOR) studies on L-α-alanine, a substantial amount of experimental data concerning electronic *g* values and hyperfine coupling constants (hfcc's) of magnetic nuclei in alanine-derived radicals is now available.

Central in the field of EPR research is the determination and interpretation of the hyperfine tensors describing the interaction between the unpaired electron(s) and nearby magnetic nuclei in the radical or neighboring radicals. Complementary to the information obtained by the available experimental techniques, quantumchemical calculations of hyperfine coupling constants (hfcc's) could be very valuable in the investigation of the electronic structure of the radicals involved and consequently in the process of elucidation of experimental EPR spectra.

Computational schemes of increasing complexity have been used with varying success to gain insight into the particular EPR spectroscopic features of radicals. Traditionally, Hückel type π orbital calculations in combination with the Heller−McConnell equations[2] have provided a way of estimating the isotropic hfcc's from the atomic unpaired spin population. However, this type of calculation does not allow for prediction of structural or geometrical features of the radicals. Semiempirical methods such as AM1[3] or INDO[4] and ab initio Hartree−Fock (HF) methods have enabled geometry optimizations and direct calculation of hfcc's. While predictions of anisotropic coupling constants are often reliable at HF level, the aforementioned methods produce inconsistent results for the isotropic hfcc's of many radicals. Furthermore, the use of restricted open-shell Hartree−Fock (ROHF) calculations is limited due to the need to account for spin polarization, e.g., for the accurate description of alpha proton hfcc's in π radicals. Unrestricted Hartree−Fock (UHF) calculations can alleviate this problem but suffer from spin contamination as the UHF wave function is not an eigenfunction of the spin operator $\mathbf{S}^2$. Due to the local nature of the Fermi contact interaction, isotropic hfcc's are very sensitive to effects such as basis set size, geometry, and electron correlation[5] and therefore necessitate an elaborate calculational scheme. This was provided by the development of high-level post-Hartree−Fock treatments (e.g., configuration interaction, coupled cluster, multiconfiguration SCF). These methods have enabled the accurate calculation of the Fermi contact interaction in radicals containing a small number of atoms.[6]

In comparison to these sophisticated ab initio techniques, the density functional theory (DFT) formalism[7] requires less computational resources with increasing system size and often yields comparable or better agreement with experiment. Both review[5,8] and regular[9−14] articles concerning the performance of DFT procedures with regard to calculations of properties of open-shell molecules in general and EPR hyperfine coupling constants in particular are available.

Radiation Chemistry of L-α-Alanine. In the numerous irradiation studies of organic crystals performed over the years, it was found that irradiation at 77 or 4 K results in entirely different species from those produced at room temperature and,

* To whom all correspondence should be addressed. Fax: 32 (0)9 264 66 99. E-mail: Philippe.Lahorte@rug.ac.be.
† Department of Subatomic and Radiation Physics, Gent University.
‡ Eenheid Algemene Chemie (ALGC), Free University of Brussels.
§ Laboratory for Crystallography and Study of the Solid State, Gent University.
⊥ Postdoctoral Fellow of the Fund for Scientific Research-Flanders (Belgium) (F.W.O.).
∥ Research Assistant of the Fund for Scientific Research-Flanders (Belgium) (F.W.O.).
⊗ Research Director of the Fund for Scientific Research-Flanders (Belgium) (F.W.O.).

10.1021/jp990942u CCC: $18.00
Published on Web 07/30/1999

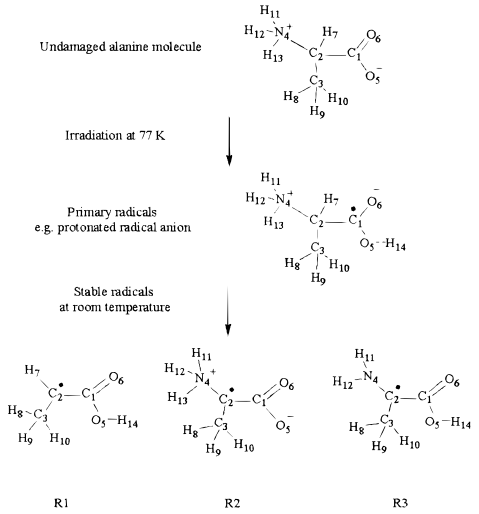

Figure 1. L-α-Alanine and derived radicals studied in this work.

furthermore, that stable radicals are formed as secondary products from the initial unstable species. The main primary process induced by ionizing radiation is the ejection of an electron from a molecule, effectively creating molecular cations, followed by electron capture and the formation of a molecular anion. Both ionic species, which are in principle detectable by EPR as paramagnetic centers, are stabilized at low temperatures and give rise at higher temperatures to an oxidative and reductive chain of radical reactions, respectively. The created neutral radicals are finally stabilized at room temperature or disappear, e.g., by recombination.

While in many cases detailed knowledge on intermediate reaction steps leading to the final products is often lacking, the initial steps can be characterized as proton donation of the positive primary ion to a neighboring molecule and proton acceptance by the negative primary ion.

This can also be demonstrated in the case of L-alanine. Its solid-state radiation chemistry is complex, involving a long series of radical transformations and reactions in both the oxidative and reductive chain of processes. From an EPR viewpoint, the stable radicals formed in the oxidative pathway are most important. Somewhat simplified, the main reactions in this chain can be summarized as follows. As alanine exists in the zwitterionic form in the crystal lattice, its molecular anion should have the structure $CH_3CH(N^+H_3)C^{\bullet}OO^{2-}$. However, it was shown that the observed spectrum originates from the protonated structure, giving rise to the primary radical anion as shown in Figure 1.[15,16] When gradually warming the irradiated crystal, the anion radical degrades by deamination, turns into an unstable radical conformation at approximately 150 K[17] and finally to a stable radical conformation at approximately 220 K.[18,19] Both the stable and the energetically more unstable radical have the same chemical structure, $CH_3C^{\bullet}HCOO^-$, as represented in Figure 1, but differ with respect to their relative orientation in the crystal lattice and internal bond lengths and angles. According to the model of Itoh and Miyagawa, the EPR absorption is to be interpreted in terms of the statistical average of the two types of radicals.[20]

While it has been commonly assumed that the room-temperature EPR spectrum of polycrystalline alanine could be ascribed to the radical R1[15,22] there have been speculations on the possible coexistence of several stable radical species,[17,18] possibly originating from other primary radicals than the one presented in Figure 1. Only recently, Sagstuen et al. presented substantial experimental evidence for the existence of a stable secondary radical R2 in irradiated alanine, contributing substantially to its room-temperature EPR spectrum.[23] In the same study, a third minority radical species was identified in the alanine spectrum which was tentatively suggested to be the species R3. The structure of both radicals is presented in Figure 1. The compositeness of the alanine powder spectrum was recently also analyzed by Vanhaelewyn et al. using heated and high-temperature X-irradiated alanine powder with a high-temperature cavity and a multivariate statistical decomposition method.[24]

Already a number of properties of alanine, e.g., basic peptide conformational stabilities,[25] gas-phase proton affinities,[26] proton chemical shifts,[27] and vibrational frequencies[28] have been investigated theoretically. In all of these studies resort was sought to DFT calculations combined with a post-Hartree−Fock method. To the best of our knowledge no thorough quantum chemical study of EPR spectroscopic properties of alanine has yet been performed. In this work, we present the results of calculations of both isotropic and anisotropic hfcc's of selected nuclei in some alanine-derived radicals. These include the aforementioned primary anion radical, the room-temperature-stable alanine radical R1 and the two "candidate" room-temperature-stable radicals R2 and R3. The calculated hyperfine interaction values are compared with the available experimental data, and the current role and scope of quantumchemical calculations of EPR spectroscopic radical properties is briefly discussed.

2. Methods

Some of the present authors already investigated the performance of DFT-based methods in the calculation of a large number of atomic and molecular properties.[29] Moreover, recent studies indicate that a computational protocol consisting of a DFT procedure both for geometry optimization and single-point property determination is likely to be the method of choice when calculating isotropic hfcc's of organic radicals.[12] In this respect, all calculations in this work were performed in the Gaussian 94 program[30] using the hybrid B3LYP functional[31] in combination with either standard Pople basis sets or the larger IGLO-III basis set.[32] The latter was designed for accurate calculation of magnetic properties. More specifically, all radicals were first optimized at the B3LYP/6-31G(d) level of theory, followed by UB3LYP/6-311G(d) or UB3LYP/IGLO−III single-point hfcc calculations. Unless mentioned otherwise, all computed values refer to the UB3LYP/6-311G(d) level of calculation.

The formulas for calculating hyperfine parameters, assuming an isotropic **g** tensor, are obtained from the spin Hamiltonian

$$H = g\beta_e S_z B_z - g_N \beta_N I_z B_z + SAI$$

The first two contributions are the electronic and the nuclear Zeeman terms, respectively, caused by the interaction of the magnetic field B_z and the magnetic moments of the electrons or nuclei in the system. g and g_N are the electron and nuclear magnetogyric ratios, and β_e and β_N are the Bohr and nuclear magnetons. The remaining term is the hyperfine interaction term and results from the interaction between the unpaired electrons and the nucleus ($I \neq 0$).

The 3×3 hyperfine interaction matrix **A** can be separated into an isotropic, spherically symmetric part (Fermi interaction) and dipolar, anisotropic components. The isotropic hyperfine splittings A_{iso} are related to the spin densities at the positions of the corresponding nuclei by

$$A_{iso} = \frac{2}{3}\mu_0 g\beta_e g_N \beta_N |\psi(0)|^2$$

TABLE 1: Calculated versus Experimental Hyperfine Coupling Constants for the Various Alanine-Derived Radicals; UB3LYP/6-311G(d)//B3LYP/6-31G(d) Level of Calculation (All Values Are in MHz)

		primary radical [a]			R1[b]			R2 [b]			R3[b]		
		A_{iso}	T_{xx} T_{yy} T_{zz}	A_{xx} A_{yy} A_{zz}	A_{iso}	T_{xx} T_{yy} T_{zz}	A_{xx} A_{yy} A_{zz}	A_{iso}	T_{xx} T_{yy} T_{zz}	A_{xx} A_{yy} A_{zz}	A_{iso}	T_{xx} T_{yy} T_{zz}	A_{xx} A_{yy} A_{zz}
C 1	calcd	247.9	127.6 −63.2 −64.4	375.5 184.7 183.5	−42.2	−6.8 0.9 5.9	−49.0 −41.3 −36.3	−31.6	−2.4 −0.4 1.9	−34.0 −32.0 −29.7	−23.8	−8.4 −4.6 13.0	−32.2 −28.4 −10.8
	exptl	251.4	128.3 −51.3 −77.4	379.7 200.1 174.0	−35.9 [c]		na	na		na	na		na
C 2	calcd	25.3	12.1 −5.3 −6.8	37.4 20.0 18.5	59.5	131.9 −66.1 −65.8	191.4 −6.6 −6.3	94.0	153.9 −76.4 −77.5	18.6 19.6 251.0	25.9	90.5 −45.6 −44.9	116.4 −19.7 −19.0
	exptl	na		na	na		na	na		na	na		na
H 7	calcd	54.9	8.2 −2.4 −5.8	63.1 52.5 49.1	−53.3	−30.5 −4.4 34.9 −31.8	−83.8 −57.7 −18.3 −87.9						
	exptl	52.7		na	−56.1	3.9 27.9	−52.2 −28.2						
H 8, H 9, H 10	calcd				65.7	7.8 −3.2 −4.6	73.5 62.5 61.1	68.4	8.5 −3.8 −4.7	77.0 64.7 63.8	35.8	6.5 −3.0 −3.6	42.3 32.8 32.2
	exptl	na		na	69.9	4.8 −2.3 −2.6	74.7 67.6 67.3	70.8	5.6 −2.7 −2.9	76.4 68.1 67.9	39.5	5.0 −2.2 −2.7	44.5 37.3 36.8
N 4	calcd	10.1	0.7 −0.2 −0.5	10.8 9.9 9.6				−8.0	−0.5 0.2 0.4 1.0	−8.5 −7.8 −7.6 8.3	6.0	−13.4 −12.7 26.1	−7.4 −6.7 32.1
	exptl	na		na				7.3	0.9 −1.8	8.2 5.5	na		na
H 11	calcd							80.3	10.3 −4.8 −5.5 9.5	90.6 75.5 74.8 95.8	−21.1	−14.7 −6.1 20.8	−35.8 −27.2 −0.3
	exptl	na		na				86.3	−2.7	83.6			
H 12	calcd							29.9	−6.9 11.3 −5.3 −5.9 10.7	79.4 41.2 24.6 24.0 40.9			
	exptl	na		na				30.2	−4.7 −6.1	25.5 24.1			
H 13	calcd							13.9	9.6 −4.4 −5.2 9.7	23.5 9.5 8.7 19.9			
	exptl	na		na				10.2	−4.8 −4.9	5.4 5.3			

[a] Reference 15. [b] Reference 23. [c] Experimentally, the absolute value is reported.

In this expression, μ_0 is the magnetic permeability in a vacuum and $|\psi(0)|^2$ is the probability of finding the electron at the nucleus. From the classical expression of interacting dipoles at a distance r, the anisotropic components $A_{\alpha,\beta}$ ($\alpha,\beta = x, y, z$) are derived as

$$A_{\alpha,\alpha} = \frac{\mu_0}{4\pi} g\beta_e g_N \beta_N \left\langle \frac{3\alpha^2 - r^2}{r^5} \right\rangle$$

$$A_{\alpha,\beta} = \frac{\mu_0}{4\pi} g\beta_e g_N \beta_N \left\langle \frac{3\alpha\beta}{r^5} \right\rangle$$

with the angular brackets indicating spatial integration over the electron wave function.

3. Results and Discussion

Table 1 presents an overview of experimental and calculated hfcc's of nuclei in the four alanine-derived radicals considered in this study. Anisotropic hfcc's are only mentioned in case the corresponding experimental values are available or when considered interesting for discussion.

Primary Alanine Radical. To investigate the electronic structure of the primary alanine radical as represented in Figure 1, a geometry optimization was performed of the undamaged alanine molecule, starting from the experimentally available atomic positions in the crystal structure, as determined in a neutron diffraction study.[33] This proved to be problematic as intramolecular proton transfer would occur from the amino group to the O6 oxygen atom. Therefore, the hydrogen bond

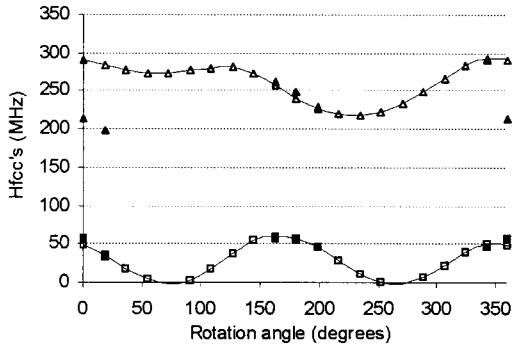

Figure 2. Angular variation of the C1 (△) and H7 (□) hfcc's upon rotation of the carboxyl group around the C1−C2 bond axis in the primary alanine radical; filled symbols [(▲) and (■)] are used to denote the respective values when performing reoptimization of all internal coordinates upon rotation; UB3LYP/6-311G(d)//B3LYP/6-31G(d) level of calculation; all values are in megahertz.

formed by O6 and an H atom of a neighboring amino group in the crystal lattice was taken into account. In a first step, a geometry optimization was performed while the internal coordinates of the two oxygen-bonded H atoms were kept frozen at the respective crystal values (bond distance O5−H14 = 1.828 Å, bond angle H14−O5−C1 = 135.3° , dihedral angle H14−O5−C1−C2 = −30.8°; bond distance O6−H = 1.861 Å, bond angle H−O6−C1 = 136.8°, dihedral angle H−O6−C1−C2 = −97.8°). As this did not result in any good agreement with experiment, a full geometry optimization was performed, followed by single-point UB3LYP/6-311G(d) level hfcc calculations at these optimized coordinates, upon rotation of the carboxyl group over 360° around the C1−C2 bond axis, in steps of 18°. As the atomic displacements upon formation of this radical are significant and isotropic hfcc's are strongly geometry dependent, the effect was examined of allowing for reoptimization of all internal coordinates for every fixed value of the dihedral angle formed by the directions of the C2−H1 bond and the lone electron orbital (LEO) situated at C1. This was done only for those rotation angles that, on the basis of the results of the calculations without reoptimization during rotation (Figure 2), seemed likely to result in a good correspondence with the available experimental values. More specifically, the region of rotation angles around 0° and 180° was investigated. At these angles, the C2−H7 bond and the LEO are respectively parallel and antiparallel to each other.

As explained by the theory of isotropic splittings at carbon centers, the magnitude of the hyperfine interaction reflects the s character of the molecular orbital occupied by the unpaired electron. In this way, the large reported experimental value of 251.4 MHz for the carboxyl carbon C1 is indicative of a deviation of planarity of the CCO_2 backbone. On the basis of empirical calculations, the authors suggested a deviation of planarity of the carboxyl group of about 8°,[15] which corresponds well with the DFT value of about 14°. This value was obtained from the radical geometries where reoptimization of all internal coordinates upon rotation of the carboxyl group was allowed. Furthermore, as can be seen in Figure 2, this "reoptimization upon rotation" procedure also confirms the fact that the only conformation where a quantitative agreement with experimental hfccs's is obtained, is for a rotation angle of 180° where the C2−H7 bond and the LEO at C1 are pointing in opposite directions. In this conformation, the direction of the LEO in our calculated model radical has rotated over 53° with respect to the direction of the LEO as calculated from the experimentally determined atomic coordinates in the undamaged molecule.[33] The corresponding calculated hfcc's are displayed in Table 1.

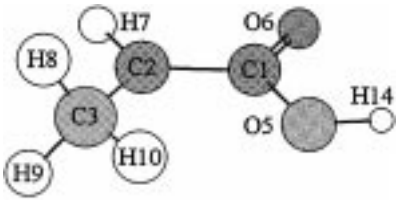

Figure 3. Ball and stick model of the B3LYP/6-31G(d) optimized structure of the radical R1.

TABLE 2: Calculated and Available Experimental Values for the Hyperfine Coupling Constants of the α Proton H7 and the Methyl Protons H8, H9, and H10 in the Radical R1; UB3LYP/6-311G(d)//B3LYP/6-31G(d) Level of Calculation (All Values Are in MHz)

H 7		H 8, H 9, H 10		
A_{iso}	A_{11} A_{22} A_{33}	A_{iso}	A_{11} A_{22} A_{33}	reference, (method, temperature)
	−87.9		74.7	
−56.1	−52.2	70.0	67.6	23 (ENDOR, 220 K)
	−28.2		67.3	
	−72.8			
−59.0	−54.9			20 (EPR, 77 K)
	−49.2			
	−88.1		71.7	
−59.8	−53.3	66.6	64.6	19 (ENDOR, 77 K)
	−37.9		63.5	
	−89.7[a]		77.1	
−53.2[a]	−46.5[a]	72.4	70.1	18 (ENDOR, 77 K)
	−23.5[a]		70.1	17 (EPR, 293 K)
	−73[a]		73	21 (EPR, 300 K,)
−60.3[a]	−57[a]	70.3	71	
	−51[a]		67	
	−83.8		73.5	
−53.3	−57.7	65.7	62.5	this work
	−18.3		61.1	

[a] Experimentally, the absolute value is reported.

The agreement with the experimental values is very good (difference < 5%). Figure 2 also displays the typical β proton character of atom H7.

Stable Alanine Radical: R1. The stick and ball model of the B3LYP/6-31G(d) optimized geometry of the radical R1 is shown in Figure 3. In their experiment with L-alanine-1-^{13}C, Sinclair and Hanna reported an essentially isotropic splitting with an absolute value of 35.9 MHz for the ^{13}C nucleus of the carboxyl group.[15] As can be seen from Table 1, these findings correlate very well with the results from the calculation.

Furthermore, our calculations confirm that the unpaired electron is primarily located at the carbon atom C2. The total atomic spin population is 0.88 and 0.89 with the 6-311G(d) and the IGLO-III basis sets, respectively. Thus, the hyperfine couplings are mainly due to interactions with the α proton H7 and the three symmetry equivalent, rotationally averaged β methyl protons. Table 2 gives an overview of the various experimentally available values for the hfcc's of the α proton and the methyl protons. The α proton interaction in the stable alanine radical R1 has been extensively investigated. As shown in Table 2, both isotropic and anisotropic calculated α proton hfcc's are in particular good agreement with the experimental values of Miyagawa et al.[18] and the ENDOR data of Sagstuen et al.[23]

Following geometry optimization of the radical, the angular variation of the methyl protons hfcc's was investigated by rotating the methyl group over 180° in steps of 18° around the C2−C3 bond axis. Figure 4A presents the results of UB3LYP/

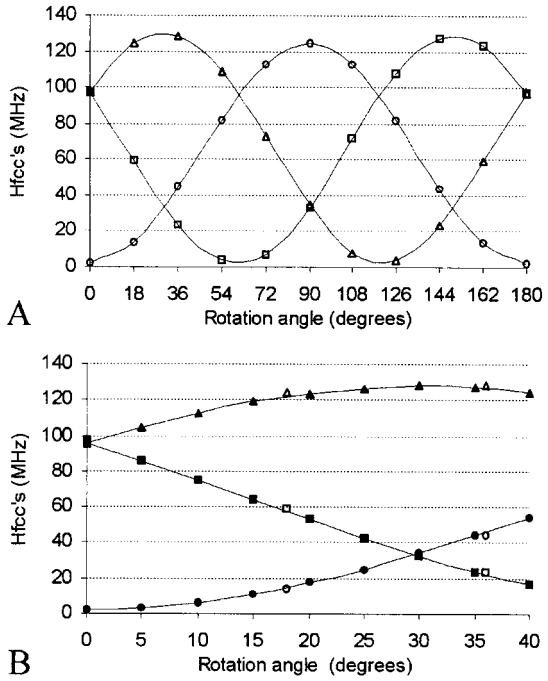

Figure 4. Angular variation of the methyl proton hfcc's upon rotation of the methyl group around the C2−C3 bond axis in the radical R1; UB3LYP/6-311G(d)//B3LYP/6-31G(d) level of calculation; all values are in megahertz: (A) using original optimized internal coordinates [(△) H8, (□) H9, (○) H10]; (B) effect of reoptimization of methyl group internal coordinates upon rotation [(▲) H8, (■) H9, (●) H10] versus using original optimized internal coordinates [(△) H8, (□) H9, (○) H10].

6-311G(d) single-point energy calculations at each conformation. From a qualitative point of view, Figure 4A clearly indicates the β proton character of the methyl protons. It has been shown in several radicals that isotropic interactions of β protons may vary considerably between approximately 10 and 140 MHz, with symmetry equivalent (i.e., rotating) protons typically showing splittings of about 70 MHz. In general, anisotropic interactions in β protons are limited. The relationship between the isotropic β proton hyperfine interaction, the 2p π spin density ρ^{π} at the atom X, and the structural parameters of a radical fragment >•X−Y−H is described by the Heller−McConnell equation,[2]

$$\alpha_{iso}^{\beta} = \rho^{\pi}(B_0 + B_2 \cos^2 \vartheta)$$

θ is the dihedral angle of the Y−H bond with respect to the plane of the LEO and X−Y bond and B_0 and B_2 are empirical parameters.

In the B3LYP/6-31G(d) optimized geometry, the radical is perfectly planar except for the two methyl protons H8 and H9 which are symmetrical to the radical plane. The dihedral angle θ of the H8−C3 and H9−C3 bond with the H10−C3 bond is 121.4° and −121.4°, respectively. Thus, in this pure π type radical, the proton H8 makes a dihedral angle θ of 31.4 degrees to the LEO at C2, which is perpendicular to the radical plane. As can be seen from Figure 4A, rotation of the methyl group over this angle toward the LEO results in a maximal contribution of H8 to the singly occupied molecular orbital (SOMO) and, consequently, a maximal hyperfine interaction. The slightly smaller maximal interaction of H10 is completely due to the use of the optimized internal coordinates in the single-point calculations. While for the H8 and H9 protons, the B3LYP/6-31G(d) H−C3 bond length is 1.100 Å and the H−C3−C2 bond angle 110.8°, the H10−C3 bond length and H10−C3−C2 bond angle are 1.091 Å and 111.9°, respectively. This results in a maximal isotropic hfcc of 124 MHz for H10 and 129 MHz for H8 and H9, or a relative difference of about 4%.

TABLE 3: Calculated and Experimental Methyl Proton hfcc's in the Stable Radical R1 at 77 K; UB3LYP/6-311G(d)//B3LYP/6-31G(d) Level of Calculation (All Values Are in MHz)

H 8		H 9		H 10		
A_{iso}	A_{11} A_{22} A_{33}	A_{iso}	A_{11} A_{22} A_{33}	A_{iso}	A_{11} A_{22} A_{33}	reference (method, temperature)
	129.2		84.1		19.3	
121.3	118.0	77.6	75.1	14.9	15.1	18 (EPR, 77 K)
	116.6		73.7		10.1	
	126.5		79.0		18.2	
118.5	115.4	71.3	68.0	10.8	7.3	this work
	113.6		66.8		6.9	

To eliminate potential effects arising from the use of the optimized geometry internal coordinates, reoptimization of the methyl group variables upon rotation, was performed. In 5° intervals, the methyl group was rotated around the C2−C3 axis over 40°, thus effectively comprising the region where a best fit is to be expected on the basis of the results in Figure 4A. The methyl protons bond lengths and bond angles, together with the C2−C3 bond length, were allowed to relax while keeping fixed both the respective dihedral angles H−C3−C2−C1 at 120° intervals and all other internal coordinates at their respective optimized geometry values. The results are displayed in Figure 4B. It can be seen that allowing for reoptimization of the internal coordinates, in this case, only has a very small effect (<3%) on the methyl proton hfcc's. This can be explained by the fact that, in the original geometry optimization, the terminal methyl protons experience very little influence from surrounding atoms. Therefore, all results concerning radical R2, also those already mentioned in Table 1, are based on the original optimized geometry data displayed in Figure 4A.

Combining the above-mentioned calculated spin density of 0.88 with the results of Figure 4A allows for estimation of the parameters in the McConnell relation for the methyl fragment −C3−H_3. In this way, we obtain 2.6 and 141.5 MHz for B_0 and B_2, respectively, which is in good agreement with previously calculated values.[22a] Previously estimated spin densities range from about 0.75 for the stable radical conformation[18,23] to 0.86 for the unstable conformation.[19]

As presented in Table 2, the calculated average value of 65.7 MHz for the isotropic hfcc of the methyl protons differs less than 10% from most of the experimental results. The values reported by Matsuki et al.[19] refer to the aforementioned unstable conformation of the radical R1 in the crystal lattice. In this unstable conformation, the methyl group motion is free at 77 K. In contrast, the methyl group motion is frozen at this temperature for the stable conformation, resulting in individualized hyperfine tensors for the three methyl protons. These were reported by Miyagawa and Itoh[18] and the principal values are displayed in Table 3. The calculated values reported in Table 3 are obtained as best fits of the curves in Figure 4A to these experimental values. A best fit is obtained upon rotating the methyl group over 13° toward the LEO. This results in a final angle θ of 18.4° for proton H8, which is in very good agreement with the experimental value of 17°.[18] The other best fits which can be determined from the results in Figure 4A simply arise from the symmetry equivalence of the three methyl protons. This means that, solely on the basis of consideration of the hfcc's, we can confirm the conclusion drawn from experiment

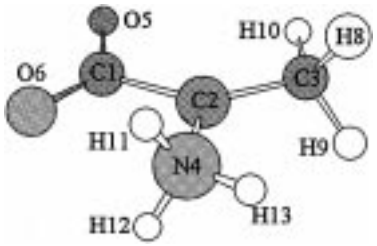

Figure 5. Ball and stick model of the B3LYP/6-31G(d) optimized structure of the radical R2.

that, in the crystal lattice, the nonrotating methyl group takes up a nonsymmetrical "skewed" configuration with respect to the plane of the radical.

Extraction of additional information concerning radical geometry and conformation would necessitate inclusion of the relevant nearest neighboring atoms in the crystal lattice and calculation and interpretation of the directions of the principal elements of the hyperfine tensors.

Radical R2. The radical R2 is formed by abstraction of the α proton in alanine. Its B3LYP/6-31G(d) geometry-optimized structure is shown in Figure 5. The UB3LYP/6-311G(d) total atomic spin density on the carbon atom C2 is 0.93 (0.96 with IGLO-III), which is substantially higher than the previously estimated value of 0.72.[23] Therefore, it is to be expected that the hyperfine interactions will be due to the methyl and amino protons. For the methyl protons, our calculations show couplings comparable to the ones in the radical R1, as shown in Table 1.

Following geometry optimization, the amino group was rotated over 180° around the N4−C2 bond axis in steps of 18°. For determination of the hfcc's of the amino protons at each of the resulting 10 conformations, single-point energy calculations at the UB3LYP/6-311G(d) level were carried out, assuming a dihedral angle of 120° between the respective amino N4−H bonds. The results are presented in Figure 6A. Analogous to the methyl protons, the amino protons display the typical β proton character, but with a smaller average isotropic coupling of 39.8 MHz. This value compares well with the experimental result of 42.2 MHz. The fact that the angular variation of the calculated hfcc's is not exactly the same for the three amino protons is again due to the use of the optimized geometry internal coordinates. Unlike proton H13, both proton H11 and H12 are attracted by the carboxyl atom O6 at the optimized geometry. The N4−H bond length for the H13 proton is 1.026 Å with a C2−N4−H bond angle of 116.2°. The respective values for the H11 and H12 protons are 1.032 Å and 106.5°. The resulting maximal isotropic hfcc for H13 is 85.0 MHz, which is roughly 10 MHz larger than the corresponding values for H11 and H12.

To eliminate these geometry effects, reoptimization of the amino group variables upon rotation was performed in an analogous procedure to the one presented in Figure 4B. The amino group was rotated over 40° around the N4−C2 axis in steps of 5°. The amino protons bond lengths and bond angles, together with the N4−C2 bond length, were allowed to relax while keeping fixed both the respective dihedral angles H−N4−C2−C1 at 120° intervals and all other internal coordinates at their respective optimized geometry values. As can be seen in Figure 6B, there is a substantial effect (approximately 10% at a rotation angle of 35°) of the reoptimization procedure for the H11 proton isotropic hfcc in the covered region of the rotation angle. Therefore, in contrast to the situation for the methyl group in radical R1, all following quantitative conclusions will be based on the results obtained using the reoptimization procedure (Figures 3C and 4B).

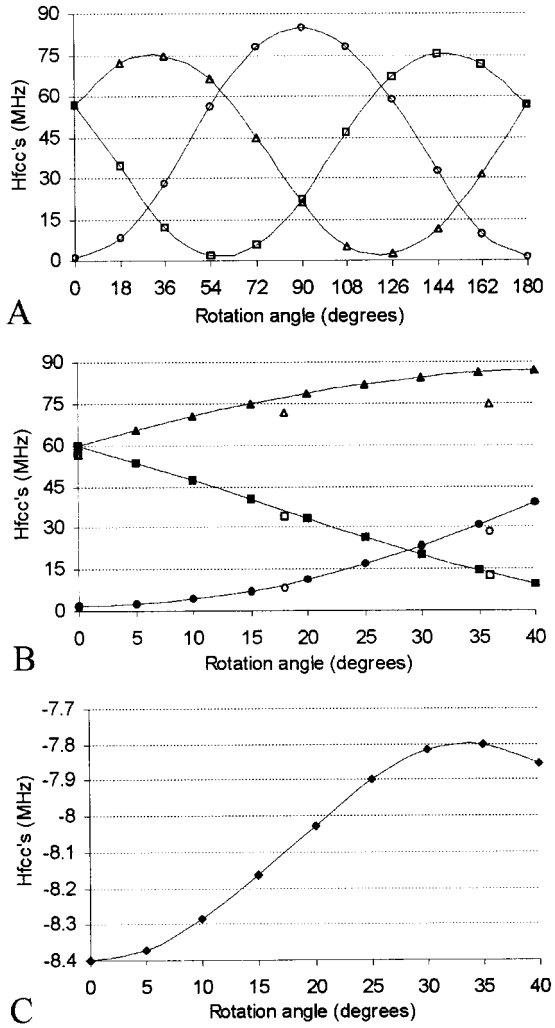

Figure 6. Angular variation of the amino proton hfcc's upon rotation of the amino group around the N4−C2 bond axis in the radical R2; UB3LYP/6-311G(d)//B3LYP/6-31G(d) level of calculation; all values are in MHz: (A) using original optimized internal coordinates [(△) H11, (□) H12, (○) H13]; (B and C) effect of reoptimization of amino group internal coordinates upon rotation [(▲) H11, (■) H12, (●) H13] versus using original optimized internal coordinates [(△) H11, (□) H12, (○) H13].

Experimentally, steric hindrance by the nearest neighboring atoms in the crystal lattice prevents the amino group from freely rotating around the N4−C2 bond axis, resulting in three individual hyperfine coupling tensors for the amino protons. A best fit of the curves in Figure 6B to the experimental values is obtained at a rotation angle of 22.4°, which results in a dihedral angle θ of the H11−N4 bond to the LEO of 7.6°. The corresponding hfcc values are presented in Table 1. The implication of our calculations for the conformation of radical R2 is that the amino group is slightly "skewed" with regard to the radical plane. This was basically also the conclusion of Sagstuen et al., who suggested a value of 7.3°, assuming perfect planarity for the radical backbone.[23]

These authors also proposed the values 8.3, 8.2, and 5.5 MHz for the principal values of the N4 nitrogen hyperfine interaction. These values were obtained by scaling down the experimental glycine values, reported by Deigen et al.,[34] by the factor 0.75/0.90 of the C2 carbon spin population and neglecting the indication of these authors for the negative sign of the actual nitrogen interaction. The variation of the N4 isotropic hfcc upon rotation of the amino group is also displayed in Figure 6C, and the rounded off values at the optimal rotation angle of 22.4°

are presented in Table 1. Our calculations confirm both the negative sign and the magnitude of the N4 atom hfcc in the alanine radical, be it with a less pronounced anisotropic character as the reported glycine values.

From the data in Figure 6B and the abovementioned calculated spin density at C2 of 0.93, the empirical parameters in the McConnell relationship can be estimated for the C2−N4−H fragment. They are 1.8 and 90.9 MHz for B_0 and B_2, respectively, which is in good agreement with available values calculated from experimental hfcc's.[35]

Radical R3. At the UB3LYP/6-311G(d) level, the total spin populations at the optimized geometry are 0.24 for the nitrogen atom N4 and 0.53 and 0.16 for the C2 and O6 atoms, respectively. Values obtained with the IGLO-III set are nearly identical. In a recent paper on glycine radicals,[36] the corresponding values were 0.18, 0.45, and 0.29 for the N4, C2, and O6 atoms, respectively. The slight differences in spin densities between atoms in radicals R1 through R3 and some of the literature data might be ascribed to the fact that those values were calculated either using the McConnell relations or a lower calculational level, semiempirical geometry (AM1 optimization) in combination with RHF-CI calculations at the INDO level. In the former case, the quality and even the validity of the empirical parameters might be questionable, while in the latter case it is clear that the quantum chemical model used in this work (DFT) is strongly different. In a recent paper on sugar radicals,[37] very similar DFT type calculations (B3LYP funtional, 6-311G(2df,p) basis sets) were used for studying sugar radicals. As in the present work, calculated spin densities of some carbon-centered radicals in that study are as high as 0.95.

As average values for the methyl protons, IGLO-III yields an isotropic hfcc of 37.1 MHz and anisotropic values of 43.5, 34.2, and 33.5 MHz. Again, these are quite comparable to the 6-311G(d) values in Table 1. Sagstuen et al. assigned two hyperfine coupling tensors for the methyl protons corresponding to two conformations of the radical R3 in the crystal lattice.[23] Next to the values given in Table 1, they also reported the respective values of 33.1 MHz for the isotropic hfcc and 37.7, 30.8, and 30.8 MHz as principal values for a second configuration of the radical R3 in the crystal lattice. Again, the agreement between experimental and theoretical values is excellent. However, the current study does not allow for investigation of the influence of the different orientation of the two radical configurations within the crystal lattice.

4. Conclusions

We have presented density functional theory calculations of isotropic and anisotropic hyperfine coupling constants of alanine-derived radicals. The theoretical coupling constants support the experimental assignment of the observed radicals. Combination of the B3LYP functional with the Pople 6-311G-(d) basis set results in proton hfcc's with a maximal deviation of about 10% from the experimental values. The IGLO-III basis set yields very similar results. Also taking into account the substantially larger computational burden, the use of the IGLO-III set is not advised for the molecular species under study.

The accuracy of the calculated carbon and nitrogen values is more difficult to assess mainly due to the lack of sufficient reliable experimental data. However, careful interpretation both of the available values for the carbon C1 in the primary radical and the radical R2 and of the nitrogen values in radical R2 leads us to believe that the 10% margin is also realistic for "heavy" atoms. To this purpose, the limitations of the current isolated molecule model may have to be overcome.

The presented results explain and support a large number of experimental observations and hypotheses about the nature and structure of radical species in irradiated alanine. They form another example of the feasibility of DFT calculations of EPR spectroscopic properties of molecular species which are of real interest to experimental scientists. However, a number of issues cannot be dealt with in the current model. For instance, atomic displacements are reported in the crystal lattice when heating the sample and one radical species transforms into another.[17,19] Experimental data also suggest that the conformation of the methyl group in R1 at 77 K and of the amino group in R2 at 220 K is deviating from trigonal symmetry.[18,23] Verification of these more subtle effects requires incorporation of the nearest neighboring molecules in the crystal lattice. Such an extended model will in principle also allow for radical geometry prediction instead of post hoc verification as in the present simulation. The investigation of these issues forms a topic of current research.

Note Added in Proof. Prior to submitting the revised version of this manuscript, a similar study as the one presented here has become available.[38] Both studies highlight different aspects of the topic under study, and the results of the overlapping parts are in close agreement.

Acknowledgment. This work has been performed in the framework of a Concerted Research Action (GOA-12050695) with financial support from the Research Board of Gent University. F. De Proft, G. Vanhaelewyn, F. Callens, and W. Mondelaers greatly acknowledge the F.W.O. Flanders (Belgium).

Supporting Information Available: The optimized geometries in Cartesian coordinates are available for all four radicals in the present study. This material is available free of charge via the Internet at http://pubs.acs.org.

References and Notes

(1) McLaughlin, W. L., Taylor, D. M., Eds.; ESR Dosimetry and Applications; Proceedings of the 4th International Symposium. *Appl. Radiat. Isotopes* **1996**, *47* (11).

(2) Heller, C.; McConnell, H. M. *J. Chem. Phys.* **1960**, *32*, 1535.

(3) Dewar, M.; Zoebisch, E.; Healy, E.; Stewart, J. *J. Am. Chem. Soc*. **1985**, *107*, 3902.

(4) Pople, J.; Beveridge, D.; Dobosh, P. *J. Am. Chem. Soc*. **1968**, *90*, 4201.

(5) Barone, V. *Recent Advances in Density Functional Methods*; World Scientific Publishing: Singapore, 1995; Chapter 8.

(6) (a) Eriksson, L. A.; Wang, J.; Boyd, R. J.; Lunell, S. *J. Phys. Chem.* **1994**, *98*, 792. (b) Chipman, D. M. *Theor. Chim. Acta* **1989**, *76*, 73. (c) Huang, M. B.; Suter, H. U.; Engels, B.; Peyerimhoff, S. D.; Lunell, S. *J. Phys. Chem.* **1995**, 99, 9724. (d) Malkin, V. G.; Malkina, O. L.; Eriksson, L. A.; Salahub, D. R. *Theoretical and Computational Chemistry*; Elsevier: Amsterdam, 1995; Vol. 2, Chapter XX .

(7) Kohn, W.; Sham, L. *J. Phys. Rev.* **1965**, *140*, A1133. Kohn, W.; Becke, A. D.; Parr, R. G. *J. Phys. Chem.* **1996**, *100*, 12974.

(8) Malkin, V. G.; Malkina, O. L.; Eriksson, L. A.; Salahub, D. R. *Modern Density Functional Theory: A Tool for Chemistry*; Elsevier: Amsterdam, 1995; Chapter 9.

(9) Barone, V.; Minichino, C.; Grand, A.; Subra, R. *J. Chem. Phys.* **1993**, *99*, 6787.

(10) Cohen, M. J.; Chong, D. P. *Chem. Phys. Lett*. **1995**, *234*, 405.

(11) Adamo, C.; Barone, V.; Fortunelli, A. *J. Chem. Phys.* **1995**, *102* (1), 385.

(12) Batra, R.; Giese, B.; Spichty, M.; Gescheidt, G.; Houk, K. N. *J. Phys. Chem.* **1996**, *100*, 18371.

(13) Walden, S. E.; Wheeler, R. A. *J. Phys. Chem*. **1996**, *100*, 1530.

(14) Fängström, T.; Eriksson, L. A.; Lunell, S. *J. Phys. Chem. A* **1997**, *101*, 4814.

(15) Sinclair, J.; Hanna, M. *J. Chem. Phys.* **1969**, *50* (5), 2125.

(16) Iwasaki, M.; Noda, S.; Toriyama, K. *Mol. Phys.* **1970**, *18*, 201.

(17) Kuroda, S.; Miyagawa, I. *J. Chem. Phys.* **1982**, *76* (8), 3933.

(18) Miyagawa, I.; Itoh, K. *J. Chem. Phys.* **1962**, *36*, 2157.

(19) Matsuki, K.; Miyagawa, I. *J. Chem. Phys.* **1982**, *76* (8), 3945.

(20) Itoh, K.; Miyagawa, I. J. *Mol. Struct.* **1988**, *190*, 85.
(21) Horsfield, A.; Morton, J. R.; Whiffen, D. H. *Mol. Phys.* **1961**, *4*, 425.
(22) (a) Miyagawa, I.; Gordy, W. *J. Chem. Phys.* **1960**, *32*, 255. (b) Morton, J. R.; Horsfield, A. *J. Chem. Phys.* **1961**, *35*, 1142. (c) Horsfield, A.; Morton, J. R.; Whiffen, D. H. *Mol. Phys*. **1962**, *4*, 425. (d) Horsfield, A.; Morton, J. R.; Whiffen, D. H. *Mol. Phys.* **1962**, *5*, 115. (e) Sinclair, J. W.; Hanna, M. W. *J. Phys. Chem*. **1967**, *71*, 84. (f) Muto, H.; Iwasaki, I. *J. Chem. Phys.* **1973**, *59*, 4821.
(23) Sagstuen, E.; Hole, E.; Haugedal, S.; Nelson, W. *J. Phys. Chem. A* **1997**, *101* (50), 9763.
(24) Vanhaelewyn, G.; Mondelaers, W.; Callens. F. *Radiat. Res*., in press.
(25) Mohle, K.; Hofmann, H. J. *J. Mol. Model*. **1998**, *4*, 53.
(26) Topol, I. A.; Burt, S. K.; Toscano, M.; Russo, N. *J. Mol. Struct*. *(THEOCHEM)* **1998**, *430*, 41.
(27) Sitkoff, D.; Case, D. A. *J. Am. Chem. Soc.* **1997**, *119*, 12262.
(28) Stepanian, S. G.; Reva, I. D.; Radchenko, E. D.; Adamowicz, L. *J. Phys. Chem. A* **1998**, *102*, 4623.
(29) (a) De Proft, F.; Martin, J. M. L.; Geerlings, P. *Chem. Phys. Lett.* **1996**, *250*, 393. (b) Geerlings, P.; De Proft, F.; Martin, J. M. L *Recent Developments in Density Functional Theory*; Elsevier: Amsterdam, 1996; Chapter 21. (c) De Proft, F.; Geerlings, P. *J. Chem. Phys*. **1997**, *106*, 3270. (d) Geerlings, P.; De Proft, F.; Langenaeker, W. *Adv. Quantum Chem*. **1999**, *33*, 303.
(30) Frisch, M. J.; Trucks, G. W.; Schlegel, H. B.; Gill, P. M. W.; Johnson, B. G.; Robb, M. A.; Cheeseman, J. R.; Keith, T.; Petersson, G. A.; Montgomery, J. A.; Raghavachari, K.; Al-Laham, M. A.; Zakrzewski, V. G.; Ortiz, J. V.; Foresman, J. B.; Cioslowski, J.; Stefanov, B. B.; Nanayakkara, A.; Challacombe, M.; Peng, C. Y.; Ayala, P. Y.; Chen, W.; Wong, M. W.; Andres, J. L.; Replogle, E. S.; Gomperts, R.; Martin, R. L.; Fox, D. J.; Binkley, J. S.; Defrees, D. J.; Baker, J.; Stewart, J. P.; Head-Gordon, M.; Gonzalez, C.; Pople, J. A. *Gaussian 94*, revision E.1; Gaussian, Inc.: Pittsburgh, PA, 1995.
(31) (a) Becke, A. D. *J. Chem. Phys.* **1993**, *98*, 5648. (b) Stevens, P. J.; Devlin, F. J.; Chablowski, C. F.; Frisch, M. J. *J. Phys. Chem*. **1994**, *98*, 11623.
(32) Kutzelnigg, W.; Fleisher, U.; Schindler, M. In *NMR−Basic Principles and Progress*; Springer-Verlag: Heidelberg, 1990; Vol. 23.
(33) Lehmann, M.; Koetzle, T.; Hamilton, W. *J. Am. Chem. Soc.* **1972**, *94* (8), 2657.
(34) Deigen, M. F.; Krivenko, V. G.; Pulatova, M. K.; Ruban, M. A.; Teslenko, V. V.; Kayushin, L. P. *Biofizika* **1973**, *18*, 235.
(35) Kohin, R.; Nadeau, P. *J. Chem. Phys*. **1966**, *44*, 691.
(36) Sanderud, A.; Sagstuen, E. *J. Phys. Chem. B* **1998**, *102*, 9353.
(37) Wetmore, S.; Boyd, R.; Eriksson, L. *J. Phys. Chem. B* **1998**, *102*, 7674.
(38) Ban, F.; Wetmore, S.; Boyd, R. *J. Phys. Chem. A* **1999**, *103*, 4303.